Talanta 96 (2012) 113–120

Contents lists available at SciVerse ScienceDirect

Talanta

journal homepage: www.elsevier.com/locate/talanta

Towards the development of a miniaturized fiberless optofluidic biosensor for glucose

David J. Cocovi-Solberg[a], Manuel Miró[a,*], Víctor Cerdà[a], Marta Pokrzywnicka[b], Łukasz Tymecki[b], Robert Koncki[b]

[a] University of the Balearic Islands, Faculty of Science, Department of Chemistry, Carretera de Valldemossa km 7.5, E-07122, Palma de Mallorca, Spain
[b] University of Warsaw, Department of Chemistry, Pasteura 1, 02-093 Warsaw, Poland

ARTICLE INFO

Article history:
Available online 18 November 2011

Keywords:
Miniaturization
Optosensor
Biosensor
Light emitting diode
Paired emitter detector diode
Sequential injection
Glucose

ABSTRACT

A miniaturized fiberless optical sensor integrated in an automated sequential injection (SI) manifold for mesofluidic handling of sample, conditioning and regeneration solutions is herein proposed for monitoring glucose (as a model analyte) in human serum. The optofluidic biosensor capitalizes on the co-immobilization of Prussian Blue (PB) and glucose oxidase (GOx) on a polyester film working concomitantly as a chemo- and bioreceptor. The oxidation of β-glucose at the receptor surface by GOx yields hydrogen peroxide whereby reoxidizing the reduced form of PB (the so-called Prussian White) so as to generate a deep blue color. The change in the optical properties of the film was continuously monitored by red paired emitter–detector diodes (PEDDs).

A full factorial design followed by a Doehlert matrix-based response surface was exploited for multivariate optimization of the optofluidic PB–GOx–PEDD biosensor. The most significant variables influencing sensor's response were the current powering the light emitting diode (LED) emitter and the surface concentration of GOx. The optosensor was proven rugged as the response varies by merely 5% from the optimal value whenever the GOx concentration increases or decreases by 17% or the current powering the LED by 18.5%. Under the optimized physicochemical conditions, the limits of detection and quantification at the $3s_{blank}$ and $10s_{blank}$ levels, respectively, were estimated to be 23.8 μmol L^{-1} and 79.3 μmol L^{-1}, respectively, with a dynamic working range spanning from 0.1 to 2.5 mmol L^{-1} of glucose. The trueness of the biosensor measurements was assessed with certified pathological and physiological human serum materials and compared against the spectrophotometric Trinder method. The devised enzymatic biosensor is affordable (less than 0.2€), sturdy, and versatile inasmuch as the chemical composition of the receptor and pair of LEDs might be customized at will.

1. Introduction

Glucose is a primary source of energy and plays a vital role in metabolic pathways. Hence, there is a continuous quest for reliable glucose assays in a broad variety of fields of knowledge, including largely biochemistry, food industry and clinical assays. In the medical field, (micro)devices for glucose monitoring in blood became the keystone in the diagnosis and treatment of multiple diseases and integral part of diabetes management as well [1,2]. Diabetes is a disease that approximately 200 million people suffer and approximately one-third of diabetics do not know they have this disease [3].

A great deal of effort has been devoted lately to the development of diverse novel approaches for improvement of the analytical performance of glucose assays on the basis of the exploitation of quantum dots, carbon nanomaterials and noble metal nanoparticles [4–7]. The pivotal analytical techniques for glucose sensing encompass amperometry, chemiluminescence, spectrophotometry and spectrofluorimetry [2,8–12]. While amperometric techniques are affordable, they might lack reproducibility [13,14] because of potential electrode poisoning, unless renewable surface amperometry is utilized [15]. Chemiluminescence is yet another appealing method for sensitive glucose assays [16,17]. Chemiluminogenic reagents in luminol-based reactions are, however, not environment friendly as containing transition metals working as catalyst [10,17] and benchtop sized equipment is oftentimes exploited, contrary to the actual miniaturization trends in detection science [18]. In fact, no analytical technique prevails upon others inasmuch as the analytical properties should be tailored to the actual analytical problem to be faced, e.g., expeditious analyses are desired in clinical assays, yet extremely low detection limits might not be necessary.

* Corresponding author. Tel.: +34 971172746; fax: +34 971173426.
E-mail address: manuel.miro@uib.es (M. Miró).

0039-9140/$ – see front matter © 2011 Elsevier B.V. All rights reserved.
doi:10.1016/j.talanta.2011.11.021

Enzymatic methods involving glucose oxidase (GOx) have drawn much attention for glucose monitoring because excellent substrate turnovers are afforded with no need of cofactors [1,9,10,16,17]. The reaction of GOx with β-glucose yields β-glucono-δ-lactone and hydrogen peroxide, the latter being readily probed on account of its redox properties. Beside amperometric biosensors, considerable research effort has harnessed GOx for colorimetric assays capitalized on chromogenic reagents or the change in color intensity of a redox indicator bearing film. To this end, the redox equilibrium between Prussian Blue (PB) and the reduced form thereof (the so-called Prussian White, PW) has shown a great potential for glucose biosensing in combination with immobilized oxidases [19,20] to minimize the expenses of costly enzymes and reduce waste generation within the framework of green analytical methodologies. The oxidation of PW by hydrogen peroxide showcases unrivalled chemical performance to the point of being regarded as artificial peroxidase [21]. The oxidation reaction raises a band centered at ca. 725 nm that has been monitored using large-sized benchtop spectrophotometers [19,20]. Instead, the combination of light emitting diodes (LEDs) as near monochromatic light sources and photodiodes as detection devices affords miniaturized and inexpensive photometers for monitoring the PB chemistry. Yet, LEDs as detectors are sturdier than photodiodes [22], are commercially available in a plethora of shapes including flat-faced bulbs, might be drilled with ease to house a flow-cell (the so-called cell within-LED) [23,24] and operate as spectrally selective detectors [22,25,26]. Thus, a current trend in optical detection is to exploit two LEDs as a complete photometric arrangement with no need of optical fibers, the so-called paired emitter–detector diode (PEDD) configuration [27,28].

Notwithstanding the fact that the operational principles of LEDs as detectors are known for ca. 3 decades [29] the analytical applications of PEDD devices have merely been recently reported. Shortly, the light that receives the LED disproportionates electrons and holes in the p-n junction (photoelectric effect) just in reverse of the usual way to use an LED. This effect occurs whenever the light the LED receives is equal or exceeds a given frequency (the same the LED should emit). The holes and electrons injected into the external circuit generate an electromotive force. The current generated is extremely low, and Diamond's group in Dublin resorted the time for the internal capacity of the LED to discharge as analytical signal [27,30,31]. On the other hand, Koncki's group in Warsaw measured the electromotive force as an analytical signal by resorting to a pH-meter [28] or low impedance voltmeter [32]. In those PEDD arrangements in which the current supplying the LED emitter is directly proportional to the intensity of the light illuminating the LED detector, Schockley's equation relates the latter with the electromotive force generated by the PEDD [28]. In combination with Lambert–Beer's law, a linear relationship is afforded between the electromotive force and the absorbance of the sample, and thus to the concentration of absorbing species [28,32]. Thus, the PEDD arrangement operates as a complete cuvette photometric device, yet recent efforts by Diamond's group have been devoted to extend the PEDD concept towards PEDD-based sensors for chemosensing of gaseous species [33–35].

In this work, we propose for the first time a PEDD-optofluidic bio-optrode for wet chemical assays as exemplified with the determination of glucose in biological samples with no prior sample treatment. Accommodated in a sequential injection (SI) network furnished with a high-precision syringe pump, a multiposition selection valve and autosampler, mechanization of the overall analytical procedure is proven feasible by integration of sample injection, sample delivery to the bioreceptor flow-cell and optrode regeneration in a fully enclosed setup capitalized on pressure-driven programmable flow. The co-immobilization of PB and GOx onto a single reusable sensing microzone in combination with a PEDD photometric device fostered the construction and miniaturization of a pseudo-reagentless (except for ascorbic acid as regenerator solution) optosensor. Optimized via a multivariate method for maximum optrode response, the proposed PB–GOx–PEDD configuration is aimed at reliable assays of glucose in human serum with negligible matrix interfering effects.

2. Experimental

2.1. Reagents and samples

4-(Pyrrol-1-yl)benzoic acid (Pyr-BAc), GOx from *Aspergillus niger* (129,900 U g^{-1}) and 1-ethyl-3-(dimethylaminopropyl) carbodiimide hydrochloride (EDC) were all purchased from Sigma–Aldrich (St. Louis, MO, USA). A 0.1 mol L^{-1} stock solution of glucose in deionized water was prepared weekly from crystalline α-D-glucose (Sigma). A minimum waiting time of 4 h is needed prior to use because of the mutarotation equilibrium between anomeric forms, as described elsewhere [10]. Working standards of glucose in 0.2 mol L^{-1} AcOH/AcOK buffer (pH 5) containing 0.2 mol L^{-1} KCl were prepared by stepwise dilution of the stock.

A 0.2 mol L^{-1} dihydrogen phosphate/hydrogen phosphate buffer (pH 7.2) was utilized as a carrier solution and to fill the optrode flow-cell whenever not in use for enzyme stabilization. The regeneration solution for the PB-embedded optrode film involved 10 mmol L^{-1} ascorbic acid in dihydrogen phosphate/hydrogen phosphate buffer (pH 7.2). Sterilized and lyophilized control human serum samples were used as reference materials for evaluation of matrix effects and method trueness exploration. Two different reference materials were purchased from Quimica Clinica Aplicada (Amposta, Spain), one serum with all of the chemical components at physiological human levels, and the other in the diabetic pathological level. The samples were prepared by reconstitution of lyophilized serum with 5.0 mL of deionized water, followed by gentle stirring for solution homogenization. The two reconstituted serum samples were mixed at ratios of 4:0, 3:1, 2:2, 1:3 and 0:4 to obtain five evenly distributed samples covering the entire range of physiological–pathological glucose levels. The commercial kit (Sigma) used as a reference method for the determination of glucose in serum samples was based on the spectrophotometric Trinder method, which is composed of GOx from *A. niger*, horseradish peroxidase, 4-hydroxybenzene sulfonic acid and 4-aminoantipyrine to yield a colored conjugated product (4-(*p*-benzochinonomonoimino)-phenazone). All other reagents used in this work were of analytical grade and used without further purification. All solutions were prepared in deionized water.

2.2. Biosensing film preparation

The PB film with immobilized oxidase is the bioreceptor part of the sensor. The non-electrolytic deposition of PB over a non-conductive surface has been described elsewhere [36]. Briefly, a transparent 100 μm-thick polyester film (Lumocolor® universal transparency film, Staedler®, Nürnberg, Germany) was soaked in 150 mL of solution containing 0.1 mol L^{-1} $K_3Fe(CN)_6$, 0.1 mol L^{-1} HCl and saturated with Pyr-BAc (ca. 1 mg), whereupon was subjected to UV-irradiation (Phillips TLD 18W/08 lamp) for two days. Two films were taped together back to back so as to obtain two films coated in a single face. Within the timeframe of irradiation, the hexacyanoferrate precipitates as a thin PB coating, that is, ($Fe_4[Fe(CN)_6]_3$), and the oxidative polymerization of Pyr-BAc yields a mixed organic–inorganic matrix that stabilizes the PB coating. The film is finally rinsed thoroughly with 0.1 mol L^{-1} HCl and water and dried prior to use. This PB film is capable of sensing both reducing and oxidizing species as a result of the reversible redox pair

PB/PW. The freshly prepared biosensing film contains the 'insoluble' PB form that ought to be converted to a more 'soluble' form, $KFe^{III}Fe^{II}(CN)_6$. The latter is known to have a more open and flexible structure that allows faster changes between the PB and PW forms [37]. This explains the fact that the analytical procedure should initiate with a film conditioning step to ensure a fast sensor response. It should be borne in mind that the transition to the soluble form requires potassium as extrareticular cation.

The N-substituted polypyrrole (PPyr-BAc) introduces functional carboxylic groups onto the surface of the PB film, making it ready for covalent binding of biomolecules [38]. In this work, a monomolecular layer of GOx is chemically attached to the composite film surface using a straightforward, one-step carbodiimide-based procedure. To this end, a given surface of the film was coated with a metered volume of enzyme (ca. 62 $\mu L\,cm^{-2}$) containing ca. 4 $kU\,mL^{-1}$ GOx and 10 $mg\,mL^{-1}$ EDC (or at different concentration ratios in the course of multivariate method optimization, see Section 3) and left to air dry. Special care should be taken in the experimental procedure due to the fact that solutes tend to concentrate at the edges of the liquid droplet. Once dried the film is ready to use. The oxidase is anchored to the organic composite matrix of the film with covalent bonding through a linker (ECD) thereby featuring high and stable biocatalytic activity without hindering the PB/PW film to work as a chemoreceptor for hydrogen peroxide.

2.3. Construction of the optofluidic sensor cell

To construct a miniaturized and affordable PEDD optrode flow-cell, two identical 5 mm-flat headed red LEDs (OSHR53E1A2M from Optosupply, HongKong) were glued to PVC housing (i.d.: 7.2 mm; o.d.: 10.5 mm; depth: 3.5 mm; with a centered hole for accommodation of LED) as illustrated in the sketch of Fig. 1. Two identical channels of about 1 mm in diameter and 1 mm deep were machined from the flat surface of the LED detector, followed by drilling two perpendicular channels of identical diameter through the body of the LED and plastic casing so as to work as flow inlet and outlet, respectively. Polytetrafluoroethylene (PTFE) tubes of 0.8 mm i.d. and 1.6 mm o.d. were glued to the inlet and outlet channels and Tygon® tubing of ca. 1.6 mm i.d. was used for connection with the flow network. The second LED operating as a light emitter was utilized without any mechanical modification. An elastic seal punched from a common silicone rubber was placed between the LED emitter and detector to generate a within-LED flow-through cell (see Fig. 1). The optical path and volume of the cell is tailorable at will on the basis of the rubber thickness. The sensing film is placed between the rubber seal and the emitter, with the optically active side facing towards the LED detector. The sealing of the flow-through optrode cell is accomplished by clamping the LED emitter to the cell housing. With a 1.0 mm thick rubber seal of 2.7 mm of inner punch diameter, the active sensing microzone was estimated at 5.7 mm^2 with an inner cell volume of 5.7 μL. The LED emitter was powered with adjustable constant current source consisting of a simple home-made circuitry incorporating a voltage regulator and operational amplifier. Temperature variations in the LED emitter as a result of operation and conductive cooling associated with the discontinuous flowing of solutions close to the gate might vary the resistance and, consequently, the current and light output. Notwithstanding the fact that constant voltage sources utilizing a resistor and thermistor in series might afford temperature compensation [26], constant current operation is proven to render unbiased data in our configuration as a result of fast temperature stabilization within the miniature flow-cell, steady temperature changes in the course of PEDD operation and reproducible detection timing inherent to SI.

2.4. Liquid handling setup and data acquisition system

A fully automated SI setup illustrated in Fig. 1 was exploited for mesofluidic handling of the overall solutions towards the optrode cell. The pressure-driven SI system is composed of a syringe pump (BU 4S, Crison Instruments, Alella, Spain) equipped with a 1-mL syringe (Gastight #1001, Hamilton®, Bonaduz, Switzerland), an eight port multiposition selection valve module (Crison Instruments) and a 45-position rack autosampler (MicroSampler, Crison

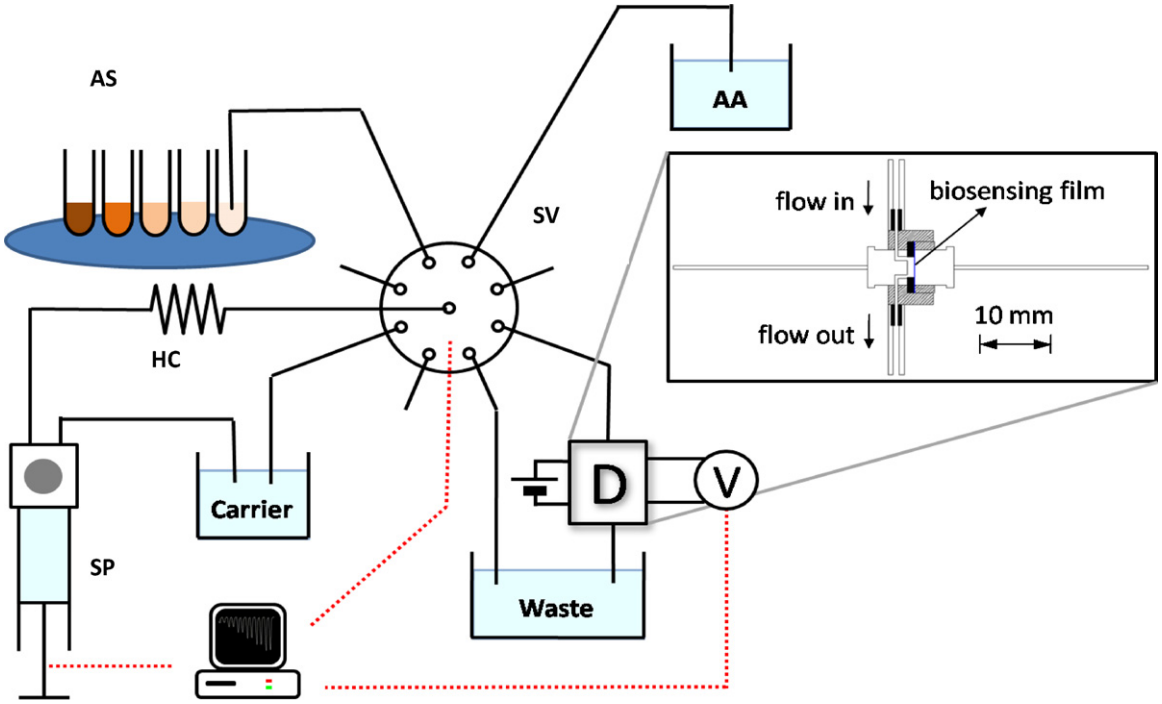

Fig. 1. Schematic illustration of the sequential injection setup integrating a miniaturized PEDD bio-optrode for automatic determination of glucose in human serum. SP: syringe pump; SV: selection valve; AS: autosampler; HC: holding coil; D: detector, AA: ascorbic acid, V: voltage. A sketch of the optofluidic sensor is shown in the inset.

Instruments). All of manifold tubing, including the 1-mL holding coil, was of PTFE with an inner diameter of 0.8 mm, excepting the connection line between the selection valve and the miniaturized biosensor with 0.5 mm of inner diameter for minimization of dead volumes and expeditious signal recording.

The electromotive force signal generated on the receptor-LED was measured with a handheld digital multimeter (Voltcraft VC820, Conrad Electronics, Hirschau, Germany) connected via an RS-232C interface to data storage PC. It should be borne in mind that the LED detector offers good sensitivity when combined with voltage readouts without the need for signal amplification. AutoAnalysis 5.0 software (Sciware, Palma de Mallorca, Spain) based on dynamic link libraries was employed for automated control of the SI instrumentation encompassing syringe pump, selection valve and autosampler, as well as for multimeter data acquisition and processing of SI-readouts. Microsoft Excel™ (Microsoft, Inc., Redmond, WA, USA) was used for statistical data treatment. Experimental design for multivariate method optimization was conducted with the aid of the computer package StatGraphics Centurion XV (Stat Point Inc., Herndon, VA, USA, 2005). Doehlert matrix-based surface response assays, signal smoothing and noise signal quantification were performed using Matlab 7.0 (MathWorks, Natick, MA, USA).

2.5. Analytical procedure

Every single working day starts with a preliminary film activation procedure, in which 150 μL of 10 mmol L^{-1} H_2O_2 in 0.2 mol L^{-1} AcOH/AcOK (pH 5.0 to avoid enzyme denaturation and enhance the oxidizing capabilities of the reagent) and 150 μL of 10 mmol L^{-1} ascorbic acid in 0.2 mol L^{-1} KH_2PO_4/K_2HPO_4 (pH 7.2) for expeditious PB reduction are sequentially carried towards the optrode flow-through cell at a flow rate of 185 μL min^{-1}. Whenever used for the first time, the above procedure is repeated 5–10-fold until sustained background signal and repeatable peak recording are obtained.

The analytical method is based on the on-line GOx catalyzed oxidation of β-glucose in heterogeneous phase to β-gluconoδ-lactone and hydrogen peroxide. The oxygen dissolved in the carrier stream at atmospheric pressure suffices for oxidation of all of the glucose, the substrate being here the limiting reactant. A buffered carrier with elevated potassium content (0.2 mol L^{-1} KH_2PO_4/K_2HPO_4, pH 7.2) is needed to overcome pH changes by protolytic species generated in the course of the enzymatic reaction and accelerate film regeneration as well [36]. For glucose sensing the PB film should be first reduced to PW, which is however chemically unstable and easily oxidized to PB. Yet, the SI setup is programmed prior to sample assays for reliable conversion of PB into PW by dispensing 400 μL of 10 mmol L^{-1} ascorbic acid to the optosensor receptor. The analytical procedure proceeds with the sequential aspiration into the holding coil of 150 μL of carrier to alleviate potential carryover effects followed by 100 μL of 10 mmol L^{-1} ascorbic acid as regenerating solution, 50 μL of carrier working as a liquid spacer and finally 700 μL of sample or glucose standard in 0.2 mol L^{-1} AcOH/AcOK at pH 5. Thereafter, the stacked composite plugs are delivered by reversed-flow to the optrode's bioreceptor surface at 185 μL min^{-1} to generate the transient signal as a result of the enzymatic oxidation of β-glucose along with the consequent oxidation of PW to PB by hydrogen peroxide generated in-line (monitored by the red LED detector at 2 Hz), followed by film regeneration to PW and baseline stabilization.

2.6. Multivariate analysis

A multivariate optimization procedure was undertaken to ascertain the effects of sample pH, current powering the LED emitter and surface GOx concentration upon PEDD-biosensor response. The criterion was to maximize the electromotive force generated by the LED detector for 1.0 mmol L^{-1} glucose. A full factorial screening design was employed to detect the main factors significantly influencing the optrode's readouts and discard the remainder from further studies [39,40]. Along with the main effects associated with individual factors, the 3 two-term interactions were calculated to explore the potential degree of twisting of the first-order planar model [41]. Whenever interactions between variables are proven to be significant, univariate (one-at-a-time) optimization methods would have led to biased results.

A lack-of-fit or curvature test [42] of the first-order model to evaluate the magnitude of predicted errors will elucidate whether or not second-order polynomial models should be selected. Whenever needed, the uniform shell, the so-called Doehlert matrix design [42,43] will be employed as a second-order model because of its efficiency in mapping space, of the exploitation of variables at different levels, and the potential reuse of experiments when the optimum is not found within the experimental domain boundaries defined at first.

3. Results and discussion

3.1. Multivariate sensor optimization

A 2^3 full factorial screening design was initially carried out at a 1 mmol L^{-1} glucose level to ascertain which factors and second-order interactions thereof have a significant influence upon sensor's response. Three potentially critical variables for the GOx-based bioreceptor and recorded analytical signal were taken into consideration, namely, the current powering the LED emitter, the pH of the reaction milieu, and the surface GOx concentration within the domain of 0.7–2.0 mA, 4.5–7.5 (using acetic acid/acetate and dihydrogen phosphate/hydrogen phosphate buffers) and 25–100 U cm^{-2}, respectively. The experimental design was built in a dimensionless coordinate system using factor coding, wherein the highest and lowest levels are given as +1 and −1, respectively, as illustrated in Table 1.

Notwithstanding the fact that each response was the averaged signal of triplicate peaks in SI-readouts, repeatability values cannot be used as estimates of the random error under intermediate precision conditions for the optrode, whereby three replicates of the central point were acquired so as to ensure that the variability found in the biosensor's response is on account of the variables selected rather than the random error [40,41]. Evaluation of the significance of factors' influence on the analytical response of the PEDD-sensor was explored using an ANOVA approach [39,41]. The standardized factor effects on glucose biosensing can be readily visualized by resorting to Pareto charts. Pareto charts are bar plots where the standardized effects being plotted are arranged in descending order and where the length of each bar is proportional to the value of a statistic *t*-test calculated for each individual factor. The positive (white) or negative (grey) bars denote those scenarios where the sensor's electromotive force signal increases

Table 1
Screening design for multivariate exploration of main variables and interactions on the PEDD microdevice response for glucose sensing.

I (mA)	pH	[GOx] (U cm^{-2})	Optrode response (mV)		
1	−1	1	31	30	30
−1	−1	1	234	227	225
−1	1	1	272	270	272
1	1	1	37	37	38
1	1	−1	5	5	5
1	−1	−1	8	7	7
−1	−1	−1	65	58	57
−1	1	−1	41	32	37

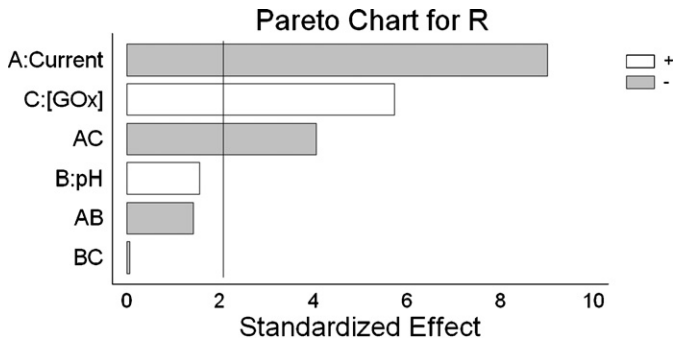

Fig. 2. Pareto chart of standardized effects ($\alpha = 0.05$) for two-level screening of the influence of main factors and two-term interactions upon bio-optrode analytical response. (A) Current powering the LED emitter; (B) sample pH; (C) GOx surface concentration. Glucose at the 1 mmol L^{-1} level. Regression equation: ΔE (mV) = 95.4 − 74.5I + 12.9pH + 47.4[GOx] − 11.8I × pH − 33.6I × [GOx] − 0.5pH × [GOx]. R = response.

or diminishes, respectively, when increasing a given factor from the lowest to the highest coded level. The Pareto chart in this work (see Fig. 2) revealed that the PEDD-powering current, the surface concentration of oxidase and their interaction are those factors that significantly influence the biosensor response at a significance level (α) of 0.05 while the reaction pH has a negligible effect within the investigated domain. The statistical significance of the interaction of LED current against concentration of GOx ($t_{exp} > t_{crit} = 2.07$) demonstrates that the univariate model commonly exploited in the investigation of analytical parameters in glucose sensors [5,13,44,45] cannot optimize the PEDD-optosensor herein proposed reliably.

The current supplying the LED emitter was proven to be the most influential and statistically significant factor in sensor's response within the investigated range of experimental conditions. If the response conforms to a first-order model the higher the current the lesser is the sensor's electromotive force signal. Powering currents approaching 2.0 mA should be avoided to preclude strong illumination of the detector for which differences between PW and PB in the sensing microzone might be negligible. Under dynamic flow conditions, the increase in GOx concentration from 25 to 100 U cm^{-2} afforded better sensor's sensitivity because of improved glucose turnover as per Pareto's chart results. The interaction between the LED powering current and the surface GOx concentration is most likely statistically significant because the optical density of the biosensitive film varies upon GOx loading. Increase in current at increasing concentration levels of immobilized enzyme is called for to offset light scattering effects.

The first-order model as predicted by the Pareto chart was, however, proven unsuitable to describe the analytical system because of curvature effects as inferred from a lack-of-fit test ($p = 0.00012 \ll 0.05$). A second-order response surface was therefore built to optimize the current powering the LED emitter and the surface GOx concentration. In a two-variable Doehlert design, one variable is explored at five levels while the other at merely three levels. In this work, the variable with the strongest effect, that is, the LED powering current, was investigated at five levels (0.20, 0.40, 0.60, 0.80, 1.0 mA) and GOx within the domain of 25–75 U cm^{-1}. Higher concentrations of oxidase are not recommended because they might hinder the free diffusion of hydrogen peroxide towards the PW film.

The response surface capitalized on Doehlert matrix was adjusted without lack-of-fit ($p = 0.44 \gg 0.05$) to a second-order polynomial model illustrated in Fig. 3 and described as follows:

$$\Delta E = -0.84 + 0.027[\mathrm{GOx}] - 0.0003[\mathrm{GOx}]^2 + 1.96I - 1.84I^2 + 0.005[\mathrm{GOx}] \times I$$

The maximum analytical response (ΔE, V) is found at 52.0 U cm^{-2} of GOx and an LED current (I) of 0.60 mA, which were selected as optimum variables for the remainder of the work. The amount of GOx entrapped in the sensing microzone (5.7 mm^2) under optimum conditions is estimated to be as small as 3 U, which is comparable with that reported lately in integrated lab-on-a-chip platforms for glucose sensing [46].

3.2. Analytical validation of the PEDD device for automated glucose optosensing

Under the optimal experimental conditions, as obtained by the Doehlert matrix multivariate method, and using a second-order polynomial regression, the dynamic working range spanned

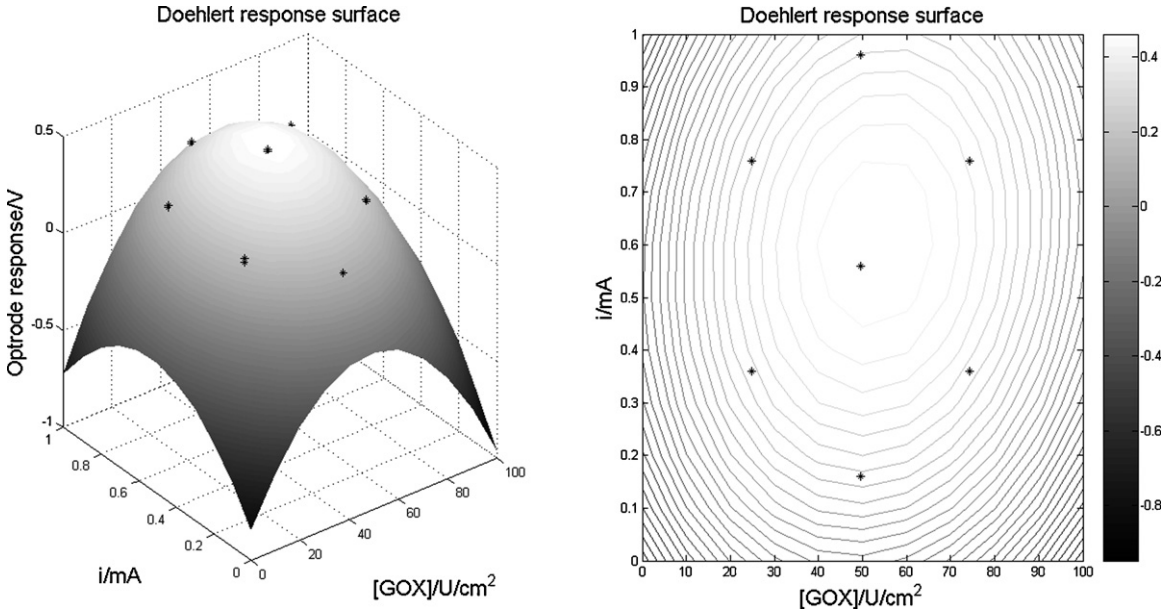

Fig. 3. Illustration of the Doehlert response surface and the contour plot as obtained from the multivariate optimization of the PEDD bio-optrode. [GOx] in U cm^{-2} and I (intensity) in mA.

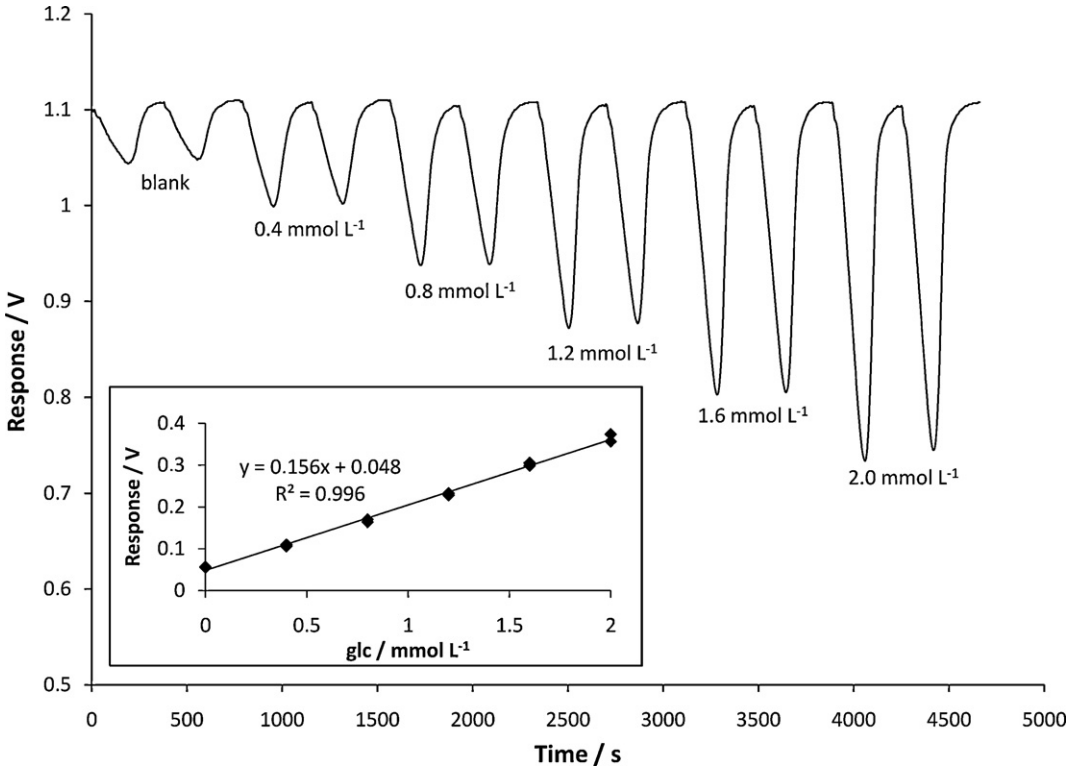

Fig. 4. Readouts of the flow-through PB–GOx–PEDD–optrode at increasing concentrations of glucose. The inset illustrates the dynamic linear range of the optosensor.

from 0.1 to 2.5 mmol L^{-1} of glucose with a coefficient of determination (R^2) of 0.9979. Increasing concentrations of substrate led to overall conversion of PW into PB. The dynamic linear range extended up to 2.0 mmol L^{-1} of glucose (ΔE (V) = 0.156 [glucose, mmol L^{-1}] + 0.048, R^2 = 0.9960, see Fig. 4) and corroborated by the lack-of-fit test ($p = 0.15 > 0.05$), which is in good agreement with earlier observations of the linearity of the PEDD response [28]. Recordings of the optrode response at increasing concentrations of glucose are illustrated in Fig. 4. The difference between the electromotive force at the baseline and peak minimum is taken as analytical signal. The upper limit of the working range may be increased at will by either increasing the flow rate of the composite zone towards the within-LED flow-cell or decreasing the sample volume injected so as to minimize the reaction time of the analyte plug with the optically active microzone. At a sample flow rate of 7.5 mL min^{-1} and using sample volumes $\leq$50 μL, concentrations of glucose up to 200 mmol L^{-1} might be analyzed without jeopardizing method repeatability.

The limits of detection (LOD) and quantification (LOQ) of glucose as per the $3s_{blank}$ and $10s_{blank}$ criteria, respectively, were estimated to be 23.8 μmol L^{-1} and 79.3 μmol L^{-1}, respectively, exploiting the least-squares regression line. The LOD is far better than that reported in a mesofluidic lab-on-a-valve platform integrating reaction and in-valve spectrophotometric detection [47], in spectrophotometric FI setups with GOx immobilized reactors [48,49] or in enzyme biosensors integrated in flow manifolds [50], all with LODs >0.055 mmol L^{-1}. Despite the minute dimensions of the flow-through cell and sensitive microzone, LOD and dynamic range of the PEDD bio-optrode are similar to SI spectrophotometric methods for glucose assays involving 10 mm pathlength cell [51].

The average S/N ratio of the PB–PEDD optrode was proven to be 3-fold better to that provided by a conventional diode-array benchtop spectrophotometer for monitoring of a PB film in 0.2 mol L^{-1} AcOH/AcOK (pH 5.0), with no need for monochromators, thus resulting in a sturdier and compact optosensor with negligible spurious radiation. The analytical signals were smothered with a Savitzky–Golay filter of second-order polynomial with a frame size of 11. The noise was then calculated as the absolute value of the analytical signal minus the smothered signal.

Method repeatability calculated as the relative standard deviation (RSD) of five consecutive assays of 1 mmol L^{-1} glucose was 2.3%. The repeatability of the PEDD biosensor is better than that previously reported in optical and electrochemical biosensors for glucose measurements with RSDs ranging from 3.5% to 6.3% [7,13,14,52]. Frequent calibrations for quality control of the bio-optrode and for compensation of potential temperature changes were readily programmed in the SI software between sample batches to correct peak heights. Because of the batchwise manufacturing process of the GOx–PB–polyester bioreceptor, calibration is recommended in individual films for improved method reliability.

Robustness or ruggedness is a property of analytical methods for which changes in system's parameters generate a negligible variation in response as compared to the optimal experimental conditions. The new PB-based PEDD optosensor herein presented was proven robust as the response varies by merely 5% whenever the surface GOx concentration increases or decreases by 17% or the current powering the LED by 18.5% from the optimal value. These values are calculated on the basis of the mathematical equation describing the Doehlert response surface.

The optosensor is designed to respond indirectly to β-glucose by sensing hydrogen peroxide through an enzymatic reaction. As a result of the reversible redox nature of the chemoreceptor, oxidizing and reducing agents in the sample medium are potential interfering species. In the presence of oxidizing agents, the color intensity of the PB film increases in comparison to that of β-glucose alone, while reducing agents diminish glucose response by reaction with hydrogen peroxide and by transformation of PB into PW at different rates on the basis of the kinetics of every single interfering species [19]. The effect of ascorbic acid in sensor response was thoroughly investigated in this work as a major interfering compound

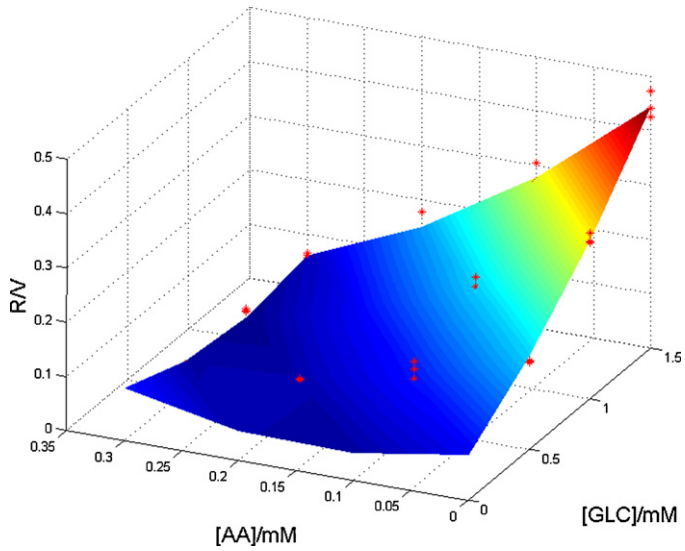

Fig. 5. 3D interference plot of PEDD-sensor response (R) against concentrations of glucose (GLC) and ascorbic acid (AA).

in serum samples. A response surface was obtained with different glucose standards (0.5, 1.0 and 1.5 mmol L^{-1}) spiked with increasing concentrations of ascorbic acid (0, 0.1, 0.2 and 0.3 mmol L^{-1}). The experimental data (see Fig. 5) were adjusted without lack-of-fit ($p = 0.17$) to a quadratic polynomial equation given below:

$$\Delta E\ (\mathrm{V}) = 0.09 + 0.13[\mathrm{glc}] - 0.54[\mathrm{AA}] + 0.07[\mathrm{glc}]^2 + 1.90\ [\mathrm{AA}]^2 - 0.88\ [\mathrm{glc}][\mathrm{AA}]$$

Glucose concentration might be thus calculated accurately once the ascorbic acid concentration is known regardless of the interference level. The critical concentration of ascorbic acid interfering at the α per one level might be estimated for each expected concentration of glucose as per the following equation:

$$[\mathrm{AA}]\mathrm{crit} = \frac{0.54 + 0.88[\mathrm{glc}] - \sqrt{(0.2916 + 0.7744[\mathrm{glc}]^2 + 0.9504[\mathrm{glc}] - 7.6\alpha(0.09 + 0.13[\mathrm{glc}] + 0.07[\mathrm{glc}]^2))}}{3.8}$$

The physiological level of glucose in human serum ranges from 4 to 8 mmol L^{-1} [2] and the mean value for ascorbic acid in human serum is ca. 28 μmol L^{-1} [53]. At a 4-fold serum dilution (*viz.*, ≥1 mmol L^{-1} glucose and 7 μmol L^{-1} ascorbic acid), the optrode response would merely decrease by ≤3.4% within the entire physiological range, i.e., the quantification of glucose at physiological level concentrations would thus be performed unbiased. Because of the specific catalytic properties of the PB/PW redox pair, the oxidation of PW by H_2O_2 at the bioreceptor surface is likely to be much faster than both the reduction of PB by ascorbic acid (film regeneration) and the reaction between ascorbate and hydrogen peroxide in the bulk solution. This observation is in good agreement with earlier reports employing optosensors with larger sensing zones [36].

To evaluate the trueness of the analytical measurements for real sample assays, five human serum reference preparations were analyzed after appropriate stepwise dilution in 0.2 mol L^{-1} AcOH/AcOK buffer (pH 5) containing 0.2 mol L^{-1} KCl, which in turn will keep ascorbic acid at non-detectable levels, using the optimized biosensor and compared against the Trinder spectrophotometric assay as a reference method. These standards cover both the physiological and diabetic pathological human concentrations (lower and upper concentrations, respectively) and three intermediate levels (see Table 2). The application of a paired *t*-test [54] revealed the inexistence of significant differences at the 0.05 confidence level ($p = 0.077$; $p > 0.05$) between the results of the PEDD–optrode and the spectrophotometric reference method. Further, improved repeatability values for pathological human serum (see standard deviation data in Table 2) were obtained by resorting to the proposed optofluidic biosensor.

Table 2
Determination of glucose (mmol L^{-1}) in human serum samples exploiting the proposed automated PEDD bio-optrode and the Trinder reference method.

	Reference range	Trinder	PEDD
A	4.88–6.55	6.6 ± 0.3	6.8 ± 0.3
B	6.50–8.75	9.5 ± 0.5	8.4 ± 0.3
C	8.39–11.32	10.7 ± 0.4	10.1 ± 0.2
D	10.14–13.71	14 ± 2	12.14 ± 0.09
E	11.90–16.10	16 ± 2	13.5 ± 0.1

Results are the mean of three replicates ± standard deviation.

In the course of the investigation maximum sensitivity conditions have been used throughout. Yet, clinical assays are aimed at maximum turnaround and/or minimum sample consumption. For the smallest flow rate in the SI setup (0.185 mL min^{-1}), the control serum volume was reduced until the S/N ratio was just above 10 for reliable quantification of the target analyte. For physiological and pathological levels, the serum volumes might be reduced down to 200 μL and 82 μL, respectively.

The sample throughput of our optrode was ca. 20 h^{-1}, which is significantly better than that reported in an earlier SI method for glucose sensing (6 h^{-1}) [51]. With regard to the increase in flow rate for a control serum volume of 700 μL, a S/N > 10 was observed for flow rates up to 2 mL min^{-1} with the subsequent increase in sample throughput up to 90 h^{-1}.

The GOx–PB–polyester sensitive layer with chemically tethered enzyme molecules showcases an excellent lifetime stability for 135 days of dry storage with a loss of enzyme activity of merely 18.8% compared to freshly cut films because the inorganic–organic composite matrix provided a biocompatible environment for the enzyme to ensure minimum protein unfolding, and prevented PB leaking as well.

Regarding stability under flow conditions, a single biosensing film could be reused for up to ca. 800 cycles of measurement and regeneration. However, daily calibration is recommended to account for slight changes in the response of the active sensing microzone.

4. Conclusion

This paper reports for the first time a PEDD-based bio-optrode involving enzymatic reactions. The optosensor is affordable (<0.20€), uses merely 3 units of enzyme and is of facile manufacture and assembly by non-skilled operators. The receptor involved a polyester film modified with PB and covalently immobilized oxidase by resorting to the EDC method. Thus, the present method provides a promising platform for the development of new enzymatic biosensors and bioelectronic devices.

The miniaturized sensor integrated in an SI manifold for handling of solutions via user-friendly programmable flow has been harnessed for assays of glucose as model analyte featuring an LOD of 23.8 μmol L^{-1}, and repeatability values of 2.3%. The most significant experimental variables upon bio-optrode response were optimized using a multivariate Doehlert matrix method. Glucose from healthy and diabetic disease individuals was successfully determined in a fully mechanized mode in control serum reference materials without any preliminary cumbersome sample pretreatment (only

dilution), thereby giving a good prospect for a new clinical device with potential applicability in point-of-care diagnosis of diabetes.

Notwithstanding the fact that computer connection is needed for sensor's proper operation and signal processing, the natural evolution of PEDD-optrode microdevices to portability is expected to be capitalized on electronic design and firmware programming to incorporate low-power microcontrollers and displays [18] and solar (battery)-powered liquid drivers.

Research work is underway in our laboratory so as to design a differential bio-optrodic device consisting of one optrode sensing glucose and the other interfering species (e.g., ascorbic acid) on the basis of PB–GOx and PB bare sensitive layers, respectively, exploiting the mathematical model described in the bulk of the text. We are also working on the automation of the electrochemical regeneration of the PW for attaining a fully-reagentless reversible biosensor.

Acknowledgments

David J. Cocovi-Solberg thanks the University of the Balearic Islands for allocation of a Ph.D. stipend. Manuel Miró gratefully acknowledges the financial support of the Spanish Ministry of Science and Innovation (MICINN) through project CTM2010-17214. Víctor Cerdà is grateful to MICINN for supporting project CTQ2010-15541. This work was also partially supported by the Polish Ministry of Science and Education (grant IP2011-043271).

References

[1] N.S. Oliver, C. Toumazou, A.E.G. Cass, D.G. Johnson, Diabet. Med. 26 (2009) 197–210.
[2] S.K. Vashist, D. Zheng, K. Al-Rubeaan, J.H.T. Luong, F.-S. Sheu, Anal. Chim. Acta 703 (2011) 124–136.
[3] http://diabetes.niddk.nih.gov/dm/pubs/statistics/index.aspx#dud (last accessed on 31.10.2011).
[4] M. Hu, J. Tian, H.-T. Lu, L.-X. Weng, L.-H. Wang, Talanta 82 (2010) 997–1002.
[5] X.-L. Wang, Y. Zhang, C.-C. Cheng, R.-R. Donga, J.-C. Hao, Analyst 136 (2011) 1753–1759.
[6] A.M. Parra-Alfambra, E. Casero, M.A. Ruiz, L. Vázquez, F. Pariente, E. Lorenzo, Anal. Bioanal. Chem. 401 (2011) 883–889.
[7] W.-J. Li, R. Yuan, Y.-Q. Chai, Talanta 82 (2010) 367–371.
[8] S. Park, H. Boo, T.D. Chung, Anal. Chim. Acta 556 (2006) 46–57.
[9] E. Wilkins, P. Atanasov, Med. Eng. Phys. 18 (1996) 273–288.
[10] N. Pizà, M. Miró, J.M. Estela, V. Cerdà, Anal. Chem. 76 (2004) 773–780.
[11] V. Sanz, S. de Marcos, J. Galbán, Talanta 78 (2009) 846–851.
[12] O. Wolfbeis, M. Schäferling, A. Dürkop, Microchim. Acta 143 (2003) 221–227.
[13] M. Piano, S. Serban, N. Biddle, R. Pittson, G.A. Drago, J.P. Hart, Anal. Biochem. 396 (2010) 269–274.
[14] E. Scavetta, B. Ballarin, D. Tonelli, Electroanalysis 22 (2010) 427–432.
[15] Y. Liu, H. Teng, H.-Q. Hou, T.-Y. You, Biosens. Bioelectron. 24 (2009) 3329–3334.
[16] X.-R. Zhang, A.M. García-Campaña, W.R.G. Baeyens, R.-I. Stefan, H.Y. Aboul-Enein, J.F. van Staden, in: A.M. García-Campaña, W.R.G Baeyens (Eds.), Chemiluminescence in Analytical Chemistry, Marcel Dekker, Inc., New York, 2001, pp. 574–576 (Chapter 20).
[17] M. Manera, M. Miró, J.M. Estela, V. Cerdà, Anal. Chim. Acta 508 (2004) 23–30.
[18] L.F. Capitán-Vallvey, A.J. Palma, Anal. Chim. Acta 696 (2011) 27–46.
[19] T. Lenarczuk, D. Wencel, S. Głąb, R. Koncki, Anal. Chim. Acta 447 (2001) 23–32.
[20] R. Koncki, T. Lenarczuk, A. Radomska, S. Głąb, Analyst 126 (2001) 1080–1084.
[21] A.A. Karyakin, E.E. Karyakina, L. Gordon, Electrochem. Commun. 1 (1999) 78–82.
[22] F.M. Mims III, Appl. Opt. 31 (1992) 6965–6967.
[23] M. Pokrzywnicka, D.J. Cocovi-Solberg, M. Miró, V. Cerdà, R. Koncki, L. Tymecki, Anal. Bioanal. Chem. 399 (2011) 1381–1387.
[24] C. Ugucione, A.A. Cardoso, Anal. Bioanal. Chem. 389 (2007) 1647–1650.
[25] E. Miyasaki, S. Itami, T. Araki, Rev. Sci. Instrum. 69 (1998) 3751–3754.
[26] P.K. Dasgupta, I.-Y. Eom, K.J. Morris, J.-Z. Li, Anal. Chim. Acta 500 (2003) 337–364.
[27] K.T. Lau, S. Baldwin, R.L. Shepherd, P.H. Dietz, W.S. Yerzunis, D. Diamond, Talanta 63 (2004) 167–173.
[28] L. Tymecki, M. Pokrzywnicka, R. Koncki, Analyst 133 (2008) 1501–1504.
[29] R.H. Lindsay, B.E. Paton, Am. J. Phys. 44 (1976) 188–189.
[30] M. O'Toole, K.T. Lau, D. Diamond, Talanta 66 (2005) 1340–1344.
[31] K.T. Lau, S. Baldwin, M. O'Toole, R. Shepherd, W.J. Yerazunis, S. Izuo, S. Ueyama, D. Diamond, Anal. Chim. Acta 557 (2006) 111–116.
[32] L. Tymecki, R. Koncki, Anal. Chim. Acta 639 (2009) 73–77.
[33] M. O'Toole, R. Shepherd, G.G. Wallace, D. Diamond, Anal. Chim. Acta 652 (2009) 308–314.
[34] D. Orpen, S. Beirne, C. Fay, K.T. Lau, B. Corcoran, D. Diamond, Sens. Actuators B 153 (2011) 182–187.
[35] I.M. Pérez de Vargas-Sansalvador, C. Fay, T. Phelan, M.D. Fernández-Ramos, L.F. Capitán-Vallvey, D. Diamond, F. Benito-Lopez, Anal. Chim. Acta 699 (2011) 216–222.
[36] R. Koncki, T. Lenarczuk, S. Głab, Anal. Chim. Acta 424 (2000) 27–35.
[37] H.J. Buser, D. Schwarzenbach, W. Petter, A. Ludi, Inorg. Chem. 16 (1977) 2704–2710.
[38] R. Koncki, O.S. Wolfbeis, Biosens. Bioelectron. 14 (1999) 87–92.
[39] B. Dejaegher, Y. Vander Heyden, LC–GC Eur. 21 (2008) 96–102.
[40] R. Leardi, Anal. Chim. Acta 652 (2009) 161–172.
[41] D.C. Montgomery, Design and Analysis of Experiments, 7th ed., John Wiley & Sons, New York, 2009.
[42] L.A. Sarabia, M.C. Ortiz, in: S. Brown, R. Tauler, R. Walczak (Eds.), Comprehensive Chemometrics, vol. 1, Elsevier, Oxford, 2009, pp. 345–390.
[43] S.L.C. Ferreira, W.N.L. dos Santos, C.M. Quintella, B.B. Neto, J.M. Bosque-Sendra, Talanta 63 (2004) 1061–1067.
[44] X.-D. Wang, T.-Y. Zhou, X. Chen, K.-Y. Wong, X.-R. Wang, Sens. Actuators B 129 (2008) 866–873.
[45] X.-P. Ji, J.-J. Ren, R.-X. Nia, X.-H. Liu, Analyst 135 (2010) 2092–2098.
[46] C.-J. Huang, Y.-H. Chen, C.-H. Wang, T.-C. Chou, G.-B. Lee, Sens. Actuators B 122 (2007) 461–468.
[47] C.-H. Wu, L. Scampavia, J. Ruzicka, B. Zamost, Analyst 126 (2001) 291–297.
[48] V. Vojinovic, F.M.F. Esteves, J.M.S. Cabral, L.P. Fonseca, Anal. Chim. Acta 565 (2006) 240–249.
[49] V. Vojinovic, C.R. Calado, A.I. Silva, M. Mateus, J.M.S. Cabral, L.P. Fonseca, Biosens. Bioelectron. 20 (2005) 1955–1961.
[50] M.A. Kumar, M.S. Thakur, A. Senthuran, V. Senthuran, N.G. Karanth, R. Hatti-Kaul, B. Mattiasson, World J. Microbiol. Biotechnol. 17 (2001) 23–29.
[51] K. Watla-iad, T. Sakai, N. Teshima, S. Katoh, K. Grudpan, Anal. Chim. Acta 604 (2007) 139–146.
[52] J.-H. Yu, S.-Q. Liu, H.-X. Ju, Biosens. Bioelectron. 19 (2003) 401–409.
[53] R. Sasaki, T. Kurokawa, S. Tero-Kubota, J. Gerontol. 38 (1983) 26–30.
[54] J.N. Miller, J.C. Miller, Statistics and Chemometrics for Analytical Chemistry, 5th ed., Pearson Education Ltd., Essex, UK, 2005, pp. 45–47 (Chapter 3).